Available online at www.sciencedirect.com
SCIENCE DIRECT®
ELSEVIER
Organic Electronics 4 (2003) 39–44
Organic Electronics
www.elsevier.com/locate/orgel

Data-storage devices based on layer-by-layer self-assembled films of a phthalocyanine derivative

Himadri S. Majumdar, Anirban Bandyopadhyay, Amlan J. Pal *

Department of Solid State Physics, Indian Association for the Cultivation of Science, Jadavpur, Kolkata 700 032, India

Received 18 February 2002; received in revised form 10 March 2003; accepted 9 April 2003

Abstract

An organic dye, namely nickel phthalocyanine, has been used in data-storage devices. A ''high state'' has been written by applying a voltage pulse. The state of the device has been ''read'' by applying a small probe voltage. The dye embedded in an inert polymer matrix retained the high state for more than an hour, which can be refreshed or erased at will. Hysteresis-type behaviour has been observed in the current–voltage characteristics. The space charges at the metal/semiconductor interfaces, stored under the voltage pulse, have been found to control the charge injection and hence the current in these devices. The formation of space charges near the interfaces, and relaxation have been studied in the data-storage devices. The space charges' slow relaxation process has been shown to result in the memory device applications of the semiconducting dyes.

PACS: 84.37.+q; 73.40.Sx; 73.61.Ph; 72.80.Le
Keywords: Data-storage device; Displacement current; Memory applications; Organic semiconductors; Phthalocyanines; Space charges

1. Introduction

In recent years, researches on organic semiconductors and conjugated polymers have attracted widespread interest due to their applications in optical and electronic devices [1]. In light-emitting diodes (LEDs), the device current is generally dominated by either charge injection or bulk transport [2]. In this respect, the studies of current–voltage–(electro)luminance characteristics under CW and transient modes showed that the space and trapped charges have an utmost important role in LED characteristics [2–7].

Apart from LEDs and photovoltaic cells, the conjugated organics can have further applications in switching [8–10] and memory devices [11,12]. In late sixties, as a first effort to use organic molecules in switching devices, organic dyes exhibited two conducting states [13,14]. In recent years, an associated memory effect has also been observed in devices based on organic molecules. Ma et al. observed two conducting states at the same applied voltage when a thin metal layer was embedded in the organics [10]. Such devices offered possibilities of rewritable memory applications. Recent reports in devices based on single layer of conjugated polymers show that a ''high'' and a

* Corresponding author. Tel.: +91-33-24734971; fax: +91-33-24732805.
E-mail address: sspajp@iacs.res.in (A.J. Pal).

1566-1199/03/$ - see front matter
doi:10.1016/S1566-1199(03)00007-7

"low" conductance states can be induced by applying a forward or a reverse voltage pulse, respectively [8,15]. The origin of such (induced) states has been explained in terms of influence of depletion layers at the electrode/polymer interfaces.

Selective usage of interfacial charges can also offer applications in data-storage devices. In porphyrin based devices, trapped charges under illumination have been measured for applications in information storage [16]. Recently, we have reported that one can "write" or "store" a "state" in conjugated polymer based single layer devices [11]. The material in such devices does not show any switching between conducting states. Still the device can retain the data even when the power is turned off. The state of the device can later be "read". The data in the device remained non-volatile for more than an hour. In this article, we extended our work to fabricate data-storage devices based on organic dyes. The use of dye molecules to fabricate such devices is itself of interest. The material's capability to retain the data, and the space charges' relaxation dynamics have been studied. Instead of conventional spin-cast or vacuum-evaporated films, layer-by-layer sequential adsorption or electrostatic self-assembled (ESA) films have been used in this work. This technique, initially introduced by Decher et al. [17], and later developed by Rubner's group [18] offers many advantages over other methods of film deposition.

2. Experiment

The dye of interest in this work is nickel(II) phthalocyaninetetrasulphonic acid, tetrasodium salt (NiPc), whose molecular structure is shown in the inset of Fig. 1. The dye and poly(allylamine hydrochloride) (PAH) (molecular weight = 70,000) were obtained from Aldrich Chemical Co. Both the chemicals were used without further purification. Indium tin oxide (ITO) coated glass substrates were used for film depositions. The substrates were cleaned following standard protocol [18].

5×10^{-3} M aqueous solutions of NiPc and PAH were made in 18 MΩ Millipore water (based on the repeat unit of the polymer). The NiPc solution served as anion, while PAH acted as polycation during the ESA film deposition. The pHs of the polycationic and the anionic solutions were adjusted to 7.5 and 3.5 by adding NaOH or HCl, respectively. Thoroughly cleaned ITO-coated glass substrates were immersed in the polycation solution for 15 min followed by rinsing in three water baths for 2, 1 and 1 min, respectively. The substrates were then immersed in the anion solution for 15 min followed by the same rinsing protocol. Each layer is deposited due to electrostatic attraction and results in surface charge reversal of the film. Deposition of a layer of polycation and a layer of anion resulted in one bilayer of ESA film, and the whole sequence has been repeated for 10 times to obtain 10 bilayer ESA films of NiPc. The films were homogeneous and are known to be stable and electrically neutral [18]. The films are further known to retain the layered nature without any ordering. Aluminium (Al) as top electrode was vacuum evaporated on the film at a pressure below 10^{-5} Torr. A mechanical mask used during Al deposition defined an active area of 6 mm^2 for each of the devices.

Current–voltage characteristics were measured with a Yokogawa 7651 dc source and a Keithley 486 picoammeter. The voltage was incremented in steps of 0.1 V. While sweeping the voltage, the

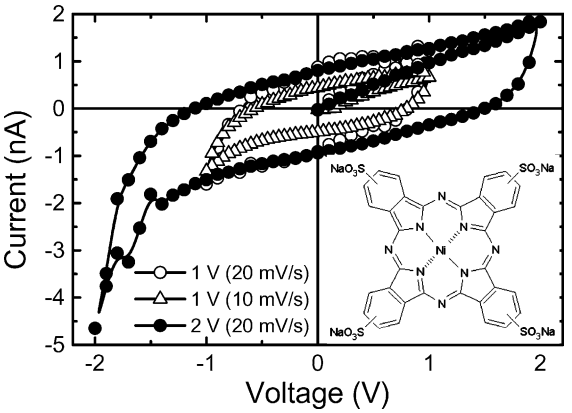

Fig. 1. Device current–applied voltage hysteresis of an ITO/NiPc/Al sandwich device. Measurements were performed at 10 and 20 mV/s sweep rates, and up to ±1 and ±2 V. Inset shows structure of NiPc.

device current was measured after allowing the current to stabilize for 10 s. The voltage-sweeps towards 0 V were initiated after a wait of 120 s at the highest voltage of sweep (a maximum of 2.5 V). Between successive measurements, the device was shorted and allowed to relax for at least 30 min. All the measurements were carried out in nitrogen environment and at room temperature. The instruments were controlled with a personal computer via a general-purpose interface bus (GPIB) interface.

3. Results and discussion

3.1. Hysteresis in current–voltage characteristics

We have recorded current–voltage characteristics (I–V) of the ITO/NiPc/Al devices in voltage loops of different amplitudes and sweep speeds. Fig. 1 shows such characteristics for 1 and 2 V loops at a sweep speed of 20 mV/s. I–V characteristics for 1 V loop have been shown for two sweep speeds. The current in all the cases show hysteresis behaviour with respect to the applied voltage. The area within the loop increased with an increase in voltage amplitude. Contribution of displacement current $\mathrm{d}(CV)/\mathrm{d}t$ in the hysteresis loop has been discussed in an earlier paper [11]. Here C represents the capacitance of the device. Fig. 1 shows that, the current amplitude at $V = 0$, the short-circuit current (I_{SC}), with sweep voltage of 2 V (during the +2 to −2 V sweep) was higher than that with sweep voltage of 1 V (during the +1 to −1 V sweep). Similarly, during the negative to positive voltage sweeps, the device current at $V = 0$ was higher when the starting sweep voltage has a higher amplitude. Since the sweep speed was 20 mV/s in both the cases, the displacement current due to voltage variation, $C(\mathrm{d}V/\mathrm{d}t)$, should be the same for a particular sweep direction. To explain higher amplitude of I_{SC} for higher amplitude of initial sweep voltage, the effect of capacitance variation has to be considered. In these devices, the contribution of capacitance variation on the displacement current $V(\mathrm{d}C/\mathrm{d}t)$ is therefore much stronger than that due to the voltage variation. Moreover, with capacitance values of these devices less than 10 nF, and a sweep speed of 20 mV/s, $C(\mathrm{d}V/\mathrm{d}t)$ amounts to a maximum of 0.2 nA, which is more than one order lower in magnitude than the device current at $V = 0$ during both sweep directions. The capacitance of the device can vary due to the formation of space charges near the semiconductor/metal interfaces, and therefore can substantially contribute to the displacement current. To understand the origin of the hysteresis behaviour in I–V plots, we therefore need to consider the role of space charges in these sandwiched devices. Feller et al. [19] have recently applied pyroelectric technique to resolve the spatial distribution of space charges in thin film. Their results also indicated a permanent storage of space charges resulting in hysteresis behaviour of pyroelectric signal with respect to the applied bias. The presence of deep-trapped charges with high time constants to reach equilibrium has also been considered for numerical simulation [20].

3.2. Formation of space charges

Formation of space charges under a voltage loop has been discussed in an earlier communication [11]. During the initial sweep from 0 to a positive voltage (Fig. 1), a layer of space charges (of holes) is established in the semiconductor near the ITO electrode. With increase in voltage, a spatial distribution of such space charges occurs. When the sweep direction was reversed (from a positive voltage to 0 V), the device retained the space charges' spatial distribution. Hence injection of charges was reduced, resulting in a decrease in device current than that during the rise of voltage. A small positive voltage, open-circuit voltage (V_{OC}), was required to balance the effect of the space charges and to maintain zero current. At zero voltage, a non-zero I_{SC} was observed. The flow of stored charges through the external circuit could give rise to such a negative I_{SC}. When the voltage was swept to reverse bias (from 0 V to a negative voltage), the current increased due to injection of holes from the Al electrode. Space charges begin to form in the layer near the Al electrode. During the reversal of direction of sweep (from a negative voltage to 0 V), these stored charges opposed injection partially and thereby

decrease the magnitude of current. During the two sweep directions the magnitudes of V_{OC} and I_{SC} were different. This might represent asymmetry in the density of stored space charges during the forward and reverse sweeps. The magnitude of current at any voltage was higher during the negative bias, as compared to that during the forward one (Fig. 1), suggesting a possible lower barrier height for charge injection in the former case.

We have compared the density of stored space charges as a function of initial sweep voltage. We have scanned I–V characteristics from different voltages to 0 V (Fig. 2). Before sweeping the voltage to 0 V, the initial voltage was applied to the device for 120 s to allow the charges to get stored in the device. The initial sweep voltage has been varied from −2 to 2.5 V, and the low-bias section of the characteristics have been shown in Fig. 2. The characteristics for the 0 to +2.5 and 0 to −2 V sweeps are also included in the figure. The current at any voltage during the 0 to $\pm V$ sweep never matched with that during the corresponding reverse sweeps ($\pm V$ to 0 V). At any forward-biased voltage, the current during the former sweep was always higher than that during the latter sweep. Moreover, with increase in initial sweep voltage, the current at a particular voltage decreased. Since the scan speed was kept the same during the $+V$ to 0 V sweeps, the displacement current due to voltage variation, however small it may be, remained the same in all the cases. The plots further show that V_{OC} and I_{SC}, whose amplitudes can be considered as measures of stored space charges in the device; increases with increase in amplitude of initial sweep voltage. This shows that more space charges can be stored by applying higher voltages amplitude.

The variation of V_{OC} and I_{SC} as a function of initial sweep voltage has been summarized in Fig. 3, where initial sweep voltage has been varied from −2 to 2.5 V. The figure shows that under forward bias the dependence is almost linear. For reverse bias, both V_{OC} and I_{SC} tend to reach a saturation. Since V_{OC} and I_{SC} could be taken as a quantitative measure of the density of stored charges, the dependences in Fig. 3 show that accumulation of space charges are asymmetric in the two bias modes. Under forward bias, the holes form space charges in the layer near the ITO electrode. Under the reverse bias, they are formed near the other electrode. When a semiconductor is sandwiched between two dissimilar metals, charge transfer occurs to align the Fermi level in the device. Holes and electrons get intrinsically accumulated in the semiconductor near the ITO and Al electrodes, respectively. Under the reverse bias, formation of positive space charges in the layer near the Al electrode may therefore become unfavourable, resulting in saturation in V_{OC} and I_{SC} with increase in amplitude of applied voltage.

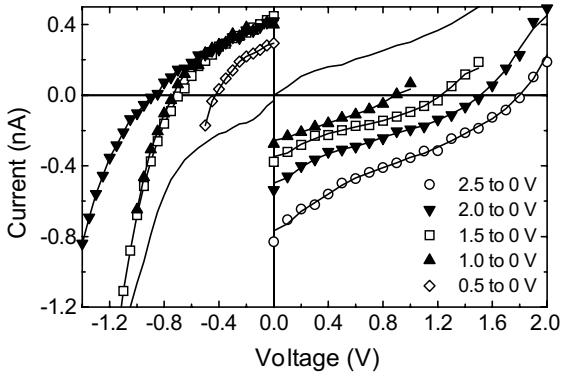

Fig. 2. Current–voltage characteristics of an ITO/NiPc/Al sandwich device at different sweep ranges. The sweep rate was 10 mV/s in all the cases. The line graphs indicate 0 V to $\pm V$ sweeps and the symbols represent $\pm V$ to 0 V characteristics.

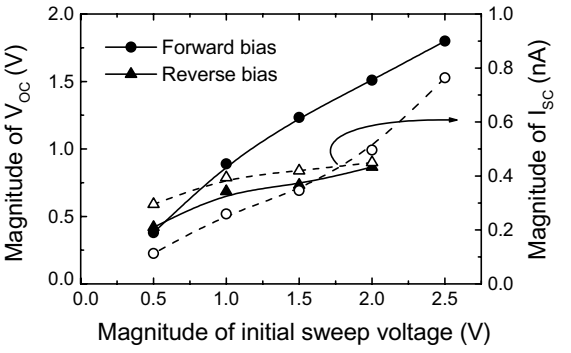

Fig. 3. Variation of the voltage magnitude at which device current becomes zero (V_{OC}) and current magnitude at $V = 0$ (I_{SC}) as a function of magnitude of initial sweep voltage for the forward and reverse bias cases. The broken lines represent I_{SC} and the lines are to guide the eye.

3.3. Relaxation of space charges

We have studied the relaxation of the space charges by pump–probe technique. A pump pulse of 3 V was applied for 5 s. After a time delay, a probe pulse of 0.2 V was applied and device current was recorded as a function of time. The time delay between the pump and the probe pulse has been varied and the device current for each of the cases have been plotted in Fig. 4. The time delay, during which the device was left open, has been varied up to 3 h. The current showed an instantaneous negative current, which decayed to a steady value. When a −3 V pump pulse was applied (not shown in the figure), the device current during the 0.2 V probe pulse showed an instantaneous positive current followed by a decay to the same steady current level. In Fig. 4, since the stored space charges resulted in the excess (negative) current, the area under the curve can represents the total amount of space charges available at that instant. The experimental results in Fig. 4 have been re-plotted in the inset to show the time dependence of available space charge. The plot depicts relaxation of the space charges under short-circuit condition by applying a low (probe) voltage pulse. The space charges can be seen to relax exponentially with time. The time constant remained the same (3 s), irrespective of the time delay between the pump and the probe pulse, and the magnitude of the pump voltage. At initial time, the decay of the space charges showed an additional fast component, which could be due to surface states induces by the pump pulse.

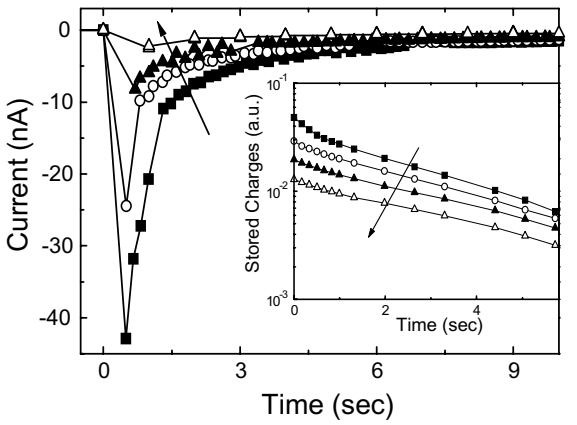

Fig. 4. Device current at 0.2 V after application of a 3 V voltage pulse (width = 5 s) as a function of time. The delays between the pump and probe pulses have been 10, 100, 300, 1800 s. Time has been measured from the beginning of the 0.2 V probe pulse. The inset shows the integral under the curve, as available space charges at different times after the 0.2 V pulse was applied. The arrows indicate the direction of increase in delay time.

3.4. Applications in memory devices

We have observed that when a voltage pulse was applied across a device, the distribution of space charges relaxed for over an hour. In Fig. 5 we have showed that the slow relaxation of stored charges in the organic dyes can make a device act in data-storage applications. To use the semiconductor in data-storage devices, we have applied a positive voltage pulse of 2 V for 5 s to write a state (say, a high state). After the application of the pump voltage pulse, the device was kept in open mode before applying a probe voltage pulse of 0.2 V for 10 s. The current during the probe pulse enabled us to read the state of the device. The probe current was measured by varying the time delay between the pump and the probe pulses. In Fig. 5, we have plotted the device current at 0.2 V probe pulse as a function of time delay. The current has been measured just before the probe voltage pulse was switched off. The current showed

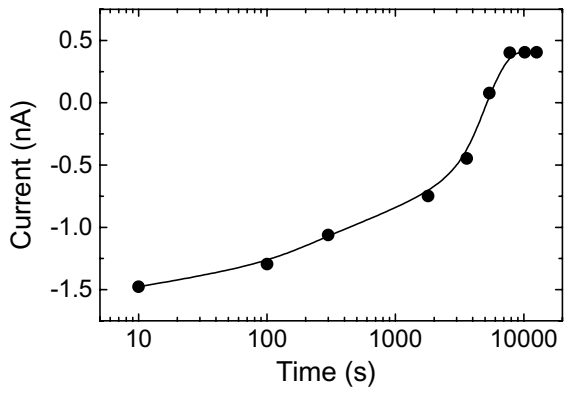

Fig. 5. Time variation of device current at 0.2 V after application of a 3 V pulse (width = 5 s). The time has been measured from the end of the 3 V pulse.

a negative value when the time delay between the pump and the probe pulses was less than 1 h. At higher time delays, the current reached a positive value, which is the value obtained in a pristine sample. The high state of the device is therefore retained for more than an hour, and the current during the probe pulse can read the state of the device. The device returns to its normal low state after an hour as evidenced by steady value of the current under the probe pulse. The sequence of this high–low state can be reproduced with ease. We could refresh the high state by applying another pump voltage pulse of same amplitude for several times. A pump voltage pulse here restores the space charge distribution of the high state in the device.

4. Conclusions

In conclusion, we have shown that organic dyes can be used in data-storage devices. In this work, we have used a derivative of nickel phthalocyanine as active semiconductor. Layer-by-layer electrostatic self-assembled films of the dye have been sandwiched between ITO and Al electrodes to fabricate the device. We have shown that one can write a high state by applying a voltage pulse. The current under a probe pulse of 0.2 V has been used to read the state of the device. The device retained the high state for more than an hour, which can be refreshed by applying another pump voltage pulse. We have studied the role of stored space charges in the data-storage or memory devices. The current–voltage characteristics showed hysteresis-type behaviour. It has been shown that space charges are stored at the active layer near the metal/semiconductor interfaces. The stored charges control charge injection through electrodes and results in the hysteresis-type current–voltage characteristics. The contributions of displacement current due to voltage variation and capacitance variation have been discussed. The density of stored charges has been compared for different voltage amplitudes of the pump pulse, and showed asymmetry during the forward and reverse biases. When shortened, the space charges in these devices have been found to relax exponentially with time with a time constant of 3 s.

References

[1] A.J. Campbell, D.D.C. Bradley, E. Werner, W. Brütting, Organic Electronics 1 (2000) 21.
[2] A.J. Campbell, D.D.C. Bradley, D.G. Lidzey, J. Appl. Phys. 82 (1997) 6326.
[3] P.W.M. Blom, M.C.J.M. Vissenberg, Mater. Sci. Eng. R 27 (2000) 53.
[4] A.J. Campbell, M.S. Weaver, D.G. Lidzey, D.D.C. Bradley, J. Appl. Phys. 84 (1998) 6737.
[5] S. Das, A.J. Pal, Appl. Phys. Lett. 76 (2000) 1770.
[6] A.J. Pal, T.P. Östergård, R.M. Österbacka, J. Paloheimo, H. Stubb, IEEE J. Sel. Top. Quant. Electron. 4 (1998) 137.
[7] W. Brütting, H. Riel, T. Beierlein, W. Riess, J. Appl. Phys. 89 (2001) 1704.
[8] D.M. Taylor, C.A. Mills, J. Appl. Phys. 90 (2001) 306.
[9] A. Bandyopadhyay, A.J. Pal, J. Phys. Chem. B 107 (2003) 2531.
[10] L. Ma, J. Liu, S. Pyo, Y. Yang, Appl. Phys. Lett. 80 (2002) 362.
[11] H.S. Majumdar, A. Bandyopadhyay, A. Bolognesi, A.J. Pal, J. Appl. Phys. 91 (2001) 2433;
Erratum, J. Appl. Phys. 91 (2002) 5508.
[12] L.P. Ma, J. Liu, Y. Yang, Appl. Phys. Lett. 80 (2002) 2997.
[13] A. Szymanski, D.C. Larson, M.M. Labes, Appl. Phys. Lett. 14 (1969) 88.
[14] A.R. Elsharkawi, K.C. Kao, J. Phys. Chem. Solids 38 (1977) 95.
[15] D. Ma, M. Aguiar, J.A. Freire, I.A. Hümmelgen, Adv. Mater. 12 (2000) 1063.
[16] C.-Y. Liu, H.-L. Pan, M.A. Fox, A.J. Bard, Science 261 (1993) 897.
[17] G. Decher, J.D. Hong, J. Schmitt, Thin Solid Films 210–211 (1992) 831.
[18] D. Yoo, S. Shiratori, M.F. Rubner, Macromolecules 31 (1998) 4309.
[19] F. Feller, D. Geschke, A.P. Monkman, Appl. Phys. Lett. 79 (2001) 779.
[20] P.H. Nguyen, S. Scheinert, S. Berleb, W. Brütting, G. Paasch, Organic Electronics 2 (2001) 105.